PAPER

Check for updates

Stochastic biosensors based on N- and S-doped graphene for the enantioanalysis of aspartic acid in biological samples†

Raluca-Ioana Stefan-van Staden, [ID] *[ab] Damaris-Cristina Gheorghe,[ab] Ruxandra-Maria Ilie-Mihai,*[a] Lucian-Barbu Tudoran[c] and Stela Maria Pruneanu[c]

Metabolomics plays a very important role in cancer mechanism and also in the early diagnosis of cancer. The enantioanalysis of aminoacids found in biological samples may favor the development of new screening tests for the early diagnosis of cancer. Two stochastic biosensors, based on the immobilization of α-hemolysin and hemin in exfoliated reduced graphene modified with nitrogen and sulphur, were proposed for the enantioanalysis of aspartic acid in biological samples (whole blood, urine, saliva, and tissue). The proposed biosensors showed low limits of quantification, high sensitivity, and large linear concentration ranges. The recoveries of D- and L-aspartic acid in biological samples were higher than 95.00%, with a relative standard deviation lower than 1.00%.

1. Introduction

Metabolic and metabolomics in gastric cancer play an important role in identifying new biomarkers such as amino acids[1–5] Cancer metabolism is based on central carbon metabolism, including glycolysis and the tricarboxylic acid cycle (the citric acid cycle, TCA cycle). Be that as it may, new surveys have revealed the significant part of amino acids in cancer metabolism. While the L-enantiomer of the chiral amino acids is usually found in the human body, the D-enantiomer may occur while the racemization process takes place or by the twisting of the DNA.

Enantioanalysis is essential when the determination of aspartic acid (Asp) is requested by the medical practitioner, because the presence of both L-Asp and D-Asp, or the absence of D-Asp may indicate different diseases. While the concentration of L-Asp is rising to μmol L^{-1} magnitude order for the patients with gastric cancer, the concentration of D-Asp is also rising to the same level, or higher, especially for patients having diseases like neuroendocrine-related diseases.[4] High plasma levels of aspartic acid were seen in old patients or patients with neurodegenerative disorders.[3,6] The changes in the serum levels of

amino acids seen in patients with gastric cancer may be firmly connected with the dietary requests of tumor cells; *i.e.*, tumor movement requires a high supplement take-up.[7]

To date, different methods were proposed for the analysis of Asp.[8] These methods include: thin layer chromatography,[9] gas chromatography,[10] high performance liquid chromatography,[11] chiral ligand-exchange capillary electrophoresis,[12] spectrophotometry,[13] fluorimetry,[14] and electrochemistry.[15] Due to the simplicity and low cost of an electrochemical method, it is necessary to develop an electrochemical system that is both highly selective and sensitive for the aspartic acid investigation. The simplicity of electrochemical techniques mixed with the small size of the apparatus and cheap instrumentation enhanced procedures, such as voltammetry, potentiometry and electrochemical impedance spectroscopy (EIS) are profoundly appealing for the location of bioactive substances.[16] In comparison with these mentioned methods, electrochemical sensors are more commonly used, due to the fact that their cost is low and they can be used with ease.[17]

To date, stochastic sensors have been used for the early diagnosis of different types of diseases, such as diabetes.[18–20] The response of the stochastic sensors is based on the channel conductivity: the first stage is the one in which the molecule enters the channel, and the current drops to zero (qualitative analysis is performed during this stage, the measured t_{off} value being known as the signature of the analyte); during the second stage, redox and binding processes take place inside the channel (the measured value of t_{on} is correlated with the concentration of the analyte). The advantages of using the stochastic sensors *versus* other electrochemical sensors are: they can perform a reliable qualitative analysis by being able to identify specific analytes, and even enantiomers; the

[a]*Laboratory of Electrochemistry and PATLAB, National Institute of Research for Electrochemistry and Condensed Matter, 202 Splaiul Independentei Str., 060021, Bucharest-6, Romania. E-mail: ralucavanstaden@gmail.com; i.ruxandra04@yahoo.com*

[b]*Faculty of Applied Chemistry and Material Science, Politehnica University of Bucharest, Bucharest, Romania*

[c]*National Institute for Research and Development of Isotopic and Molecular Technologies, Donat Street, 67-103, Cluj-Napoca, Romania*

† Electronic supplementary information (ESI) available. See DOI: 10.1039/d1ra02066h

quantitative analysis is also reliable, the quantification being performed inside the channel found in the powders used for the design of the sensor.[18–20]

In this paper, two stochastic biosensors based on α-hemolysin and hemin, immobilized in an exfoliated graphene doped with nitrogen and sulphur were proposed for the enantioanalysis of aspartic acid in biological samples: whole blood, urine, saliva, and tissue. The selection of α-hemolysin and hemin for the design of the stochastic sensors is due to the structures of α-hemolysin and hemin; α-hemolysin and hemin present the necessary pores needed for obtaining the stochastic sensing. The conductivity of the material used as matrix (graphene material): selection of N- and S-dopped graphene increased the conductivity of graphene, and also the signal/noise ratio for the stochastic sensors; no stochastic signal was obtained for the enantioanalysis of Asp when we modified plane graphene with the same biomolecules. Going from graphite material – which proved in the laboratory to be the most difficult matrix for stochastic sensors due to the instability of channels (due to the van der Waals forces taking place between the graphene layers of graphite), the graphene material was far more easy to use because of high stability of the signal, and higher reproducibility of the measurements compared with those obtained using the graphite pastes.

2.   Materials and methods

2.1.   Materials and reagents

D- and L-aspartic acid, ammonium thiocyanate (NH$_4$SCN), and ammonia were bought from Sigma Aldrich (Milwaukee, USA). Paraffin oil was bought from Fluka (Buchs, Switzerland).

Standard solutions of aspartic acid 10^{-3} mol L^{-1}, buffered with phosphate buffer, pH = 7.50 were prepared. The solutions were diluted to 10^{-16} mol L^{-1} using a serial dilution method.

2.1.1.   Electrochemical synthesis of graphene (E-NSGr). The graphene sample was obtained by electrochemically exfoliating graphite rods immersed in a solution containing 0.1 mol L^{-1} NH$_4$SCN and 0.2 mol L^{-1} ammonia (Fig. 1). Short pulses of current were applied between the two electrodes, for 4 hours. The bias (12 V) was applied through an external power supply and the time parameters e.g., pulse duration (0.8 s) and the

pause between two pulses (0.2 s) were controlled through a static switch.[21]

At the end of the exfoliation process, the material collected in the reaction vessel was washed with large amounts of water (10 L), filtered with paper to remove the large particles and finally dried by lyophilization. According to the elemental analysis, the sample had 3.99 wt% nitrogen and 1.06 wt% sulphur, and was denoted E-NSGr.

The successful integration of hetero atoms into the graphene generally requires high temperature, therefore it is of paramount importance to develop facile approaches towards the synthesis of doped graphene materials. In our case, the electrolyte based on NH$_4$SCN and ammonia will generate ions by dissociation, such as NH$_4^+$ and SCN$^-$. The ions will be electrochemically attracted towards the cathode respectively the anode, leading to the exfoliation of graphite. We suggest that the network defects formed during exfoliation may keep the ions trapped within the graphene layers, forming the NS-doped graphene.

2.2.   Apparatus and methods

All measurements were performed using an AUTOLAB/PGSTAT 302 (Metrohm, Utrecht, The Netherlands), connected to a computer on which the GPES software was installed; the computer was used to record all the measurements. In order to obtain the electrochemical set-up, three electrodes were used: the counter electrode, represented by a platinum wire, the working electrode, which in our case was represented by the stochastic biosensor and the Ag/AgCl wire, which represents the reference electrode (0.1 mol L^{-1} KCl). For this method, the values of t_{off} and t_{on} are required, therefore, a chronoamperometric method was used; moreover, a constant potential of 125 mV was applied.

The morphology of the graphene sample was investigated using the Scanning Electron Microscopy (SEM) technique (SU-8230 STEM system, Hitachi, Japan). The UV-Vis spectrum of graphene sample ultrasonically dispersed in distilled water (0.05 mg mL^{-1}) was recorded with a SPECORD 250 PLUS, Analytic Jena (Germany). The FTIR spectrum of graphene embedded in the KBr pellet was recorded with a Bruker Tensor II spectrometer (Germany) while the Raman spectrum with
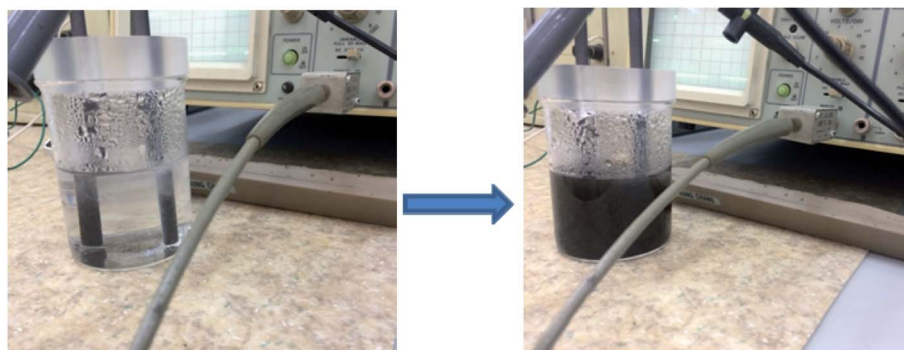

Fig. 1   Electrochemical exfoliation of graphite rods immersed in a solution containing 0.1 mol L^{-1} NH$_4$SCN and 0.2 mol L^{-1} ammonia (applied bias 12 V; pulse duration 0.8 s; the pause between two pulses 0.2 s).
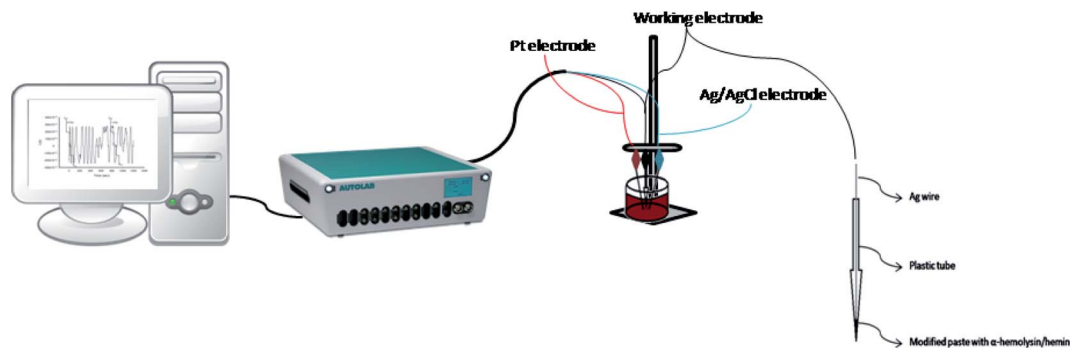
Fig. 2 The schematic diagram of the stochastic method and the design of the stochastic biosensors.

a SOLAR TII spectrophotometer coupled with an Olympus IX71 microscope. The elemental analysis of the E-NSGr sample was obtained with an Elemental Analyzer—FLASH EA 1112 (Italy).

A Christ alpha 1-4 LSC freeze dryer was used for the lyophilization of the sample.

2.3.   Design of the stochastic biosensors

The two stochastic biosensors were constructed as follows: the exfoliated graphene doped with N and S was mixed with paraffin oil in order to obtain a homogeneous paste. The homogeneous paste was split in half; one half was modified with α-hemolysin and the other half was modified with hemin, by physically mixing the graphene paste and the solution of α-hemolysin and hemin (10^{-3} mol L^{-1}), respectively. Practically, 100 mg of

graphene powder was mixed with 100 μL of α-hemolysin or hemin solution (10^{-3} mol L^{-1}). α-Hemolysin and hemin are biomolecules able to provide the pores/channels needed for the stochastic sensing. Each modified paste was placed in a non-conducting plastic tube (i.d. of 100 μm). In order to create the connection between the pastes and the external circuit, silver wires were placed inside the plastic tubes containing the modified pastes (Fig. 2). When not in use, the biosensors were kept in the fridge, at a temperature between 2–8 °C.

2.4.   Stochastic mode

The stochastic mode was employed for all measurements. All measurements were done at 125 mV $vs.$ Ag/AgCl. The

Fig. 3 Pattern recognition of D- and L-aspartic acid in biological samples using stochastic biosensors based on α-hemolysin/E-NSGr: (a) whole blood samples, (b) tissue samples, (c) urine samples and (d) saliva samples.
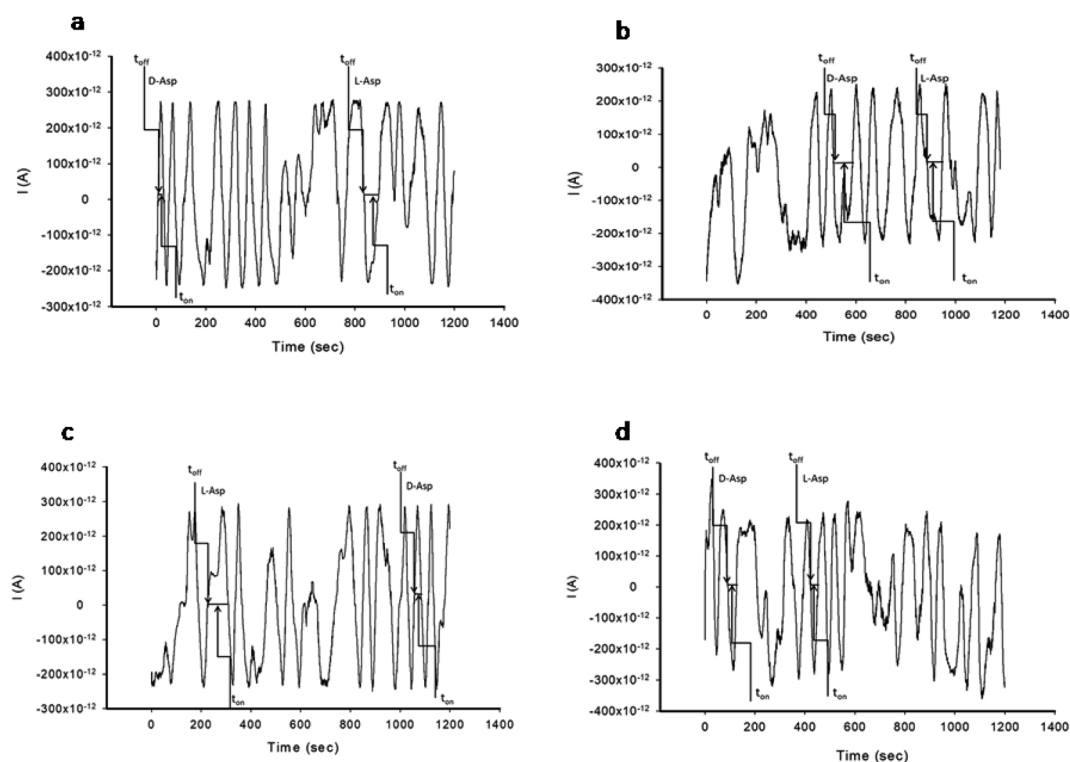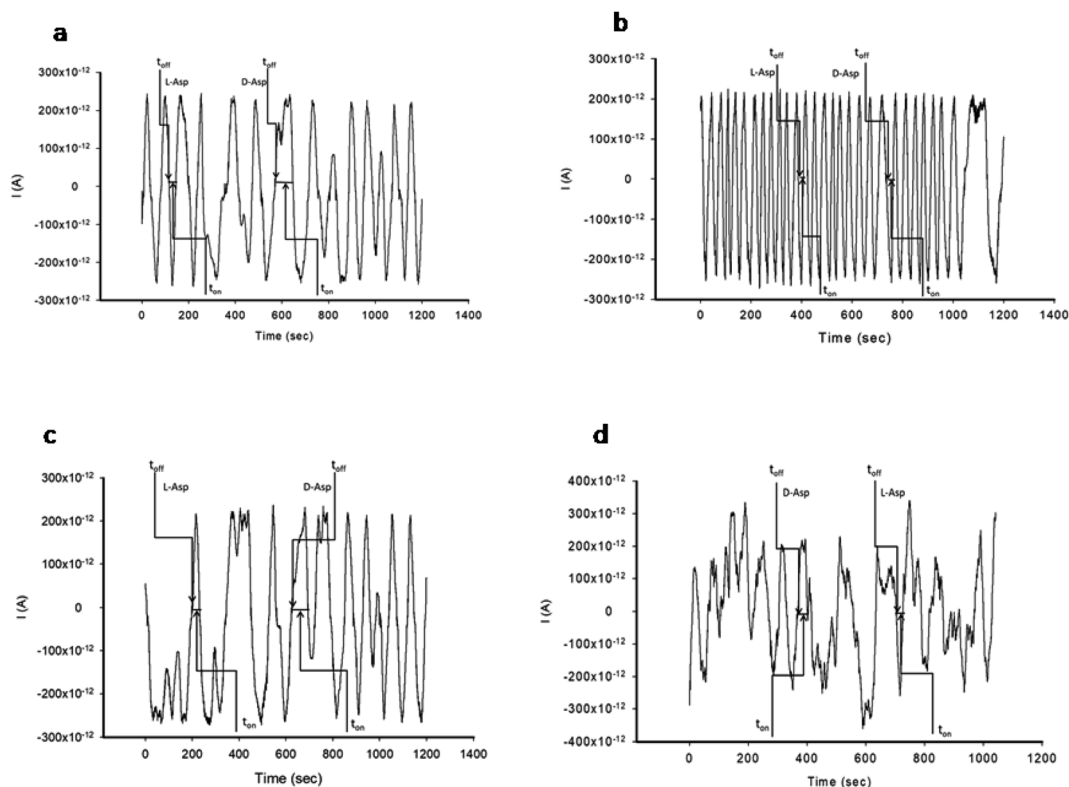
Fig. 4 Pattern recognition of D- and L-aspartic acid in biological samples using stochastic biosensors based on hemin/E-NSGr: (a) whole blood samples, (b) tissue samples, (c) urine samples and (d) saliva samples.
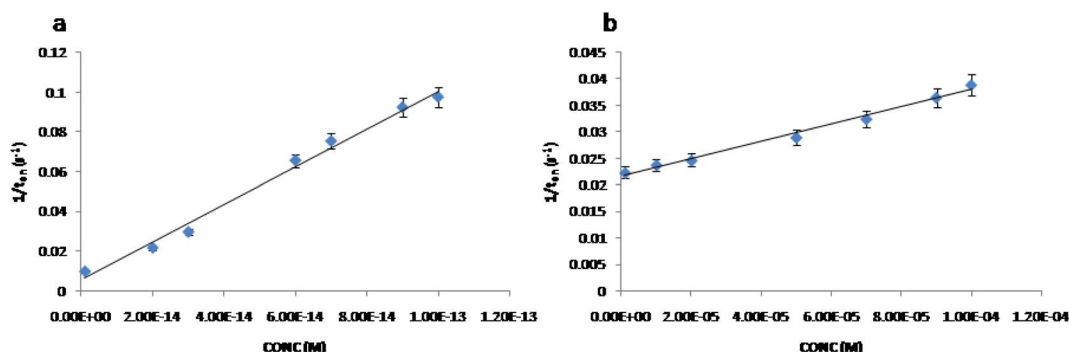

Fig. 5 The calibration curves for the biosensor modified with α-hemolysin for L-Asp (a) and D-Asp (b).

functioning of the stochastic biosensors is based on the channel conductivity.

Qualitative and quantitative enantioanalysis of Asp from whole blood, tissue, urine and saliva samples can be performed using the proposed biosensors. The parameters of interest were: t_{off} and t_{on}, respectively (Fig. 3 and 4). t_{off} is known as the signature of the analyte and is used for the qualitative analysis. t_{on} is known as the necessary time of equilibrium for the interaction of the analyte with the wall channel; this parameter is used in quantitative enantioanalysis. The equations of calibration ($1/t_{on} = a + bx\text{Conc}_{enantiomer}$) and all parameters of the sensors were obtained using the linear regression method. The unknown concentration of the enantiomer was determined by using the equation of calibration (Table 2, Fig. 5 and 6). The time needed for the calibration measurements was 360 s, while the biological samples were assayed for 1200 s.

2.5. Samples

County Emergency Hospital from Targu-Mures provided samples of whole blood, tissue, urine and saliva from confirmed patients with gastric cancer, but also from healthy patients (Ethics committee approval number 32647/2018 awarded by the County Emergency Hospital from Targu-Mures). Written consent was obtained from all patients. No sample pretreatment was performed for the samples analyzed using the proposed biosensors.
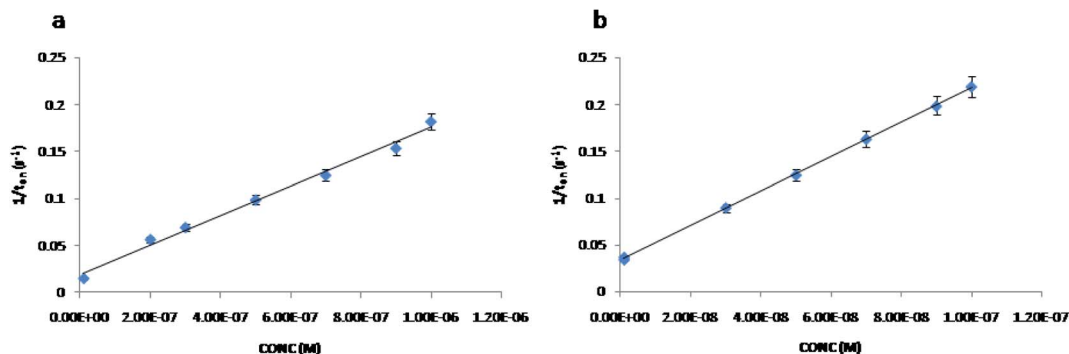
Fig. 6 The calibration curves for the biosensor modified with hemin for L-Asp (a) and D-Asp (b).
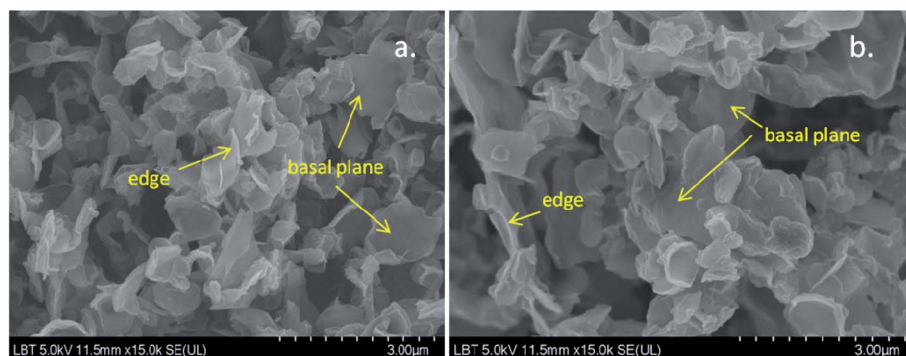

Fig. 7 Representative SEM images of the E-NSGr sample; scale bar 3 μm.

3. Results and discussions

3.1. Morphological and structural characterization of the E-NSGr sample

In Fig. 7a and b are shown representative SEM images of graphene flakes obtained after the electrochemical exfoliation of graphite rods in a solution containing 0.1 mol L^{-1} NH_4SCN and 0.2 mol L^{-1} ammonia.

Both images reveal that the sample is composed of flakes with large and smooth regions that correspond to the basal plane of graphene as well by narrow and white regions, where the edges of graphene roll up. Overall, the sample morphology is a porous one, therefore it has a large surface area, which brings many advantages when the material is employed in the electrochemical sensing of various molecules.

The structural characterization of E-NSGr was next performed by UV-Vis, FTIR, and Raman spectroscopy. In Fig. S1† one can see the UV-Vis spectrum of graphene sample previously sonicated in water for 3 minutes. The absorbance peak of graphene can be generally found at wavelengths between 250 and 300 nm, in contrast with that corresponding to graphene oxide which appears at around 230 nm. In the case of the E-NSGr sample, a strong absorption peak occurs at 275 nm which is due to the $\pi \rightarrow \pi^*$ transitions within the C=C bonds. The small shoulder around 315 nm originates from the n $\rightarrow \pi^*$ transitions within the oxygen-containing functional groups.

This indicates that the sample contains a small amount of flakes bearing oxygen groups.

The FTIR spectrum of E-NSGr (Fig. S2a and b†) further indicates the presence of vibrations corresponding to oxygen-containing groups attached to the graphene surface, such as: the strong and broad O–H stretching vibration at 3432 cm^{-1} due to the adsorbed water molecules, the O–H deformation vibration at 1386 cm^{-1}, the C–O (alcoxy) stretching vibration at 1072 cm^{-1}. The intense bands at 1400 cm^{-1} may be attributed to NH_4^+ vibration while the weaker band at 1165 cm^{-1} indicates the existence of C–N/C–S vibrations.[22]
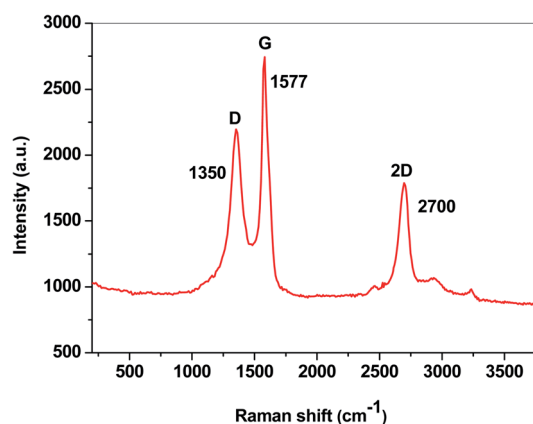

Fig. 8 The Raman spectrum of the E-NSGr sample.

Table 1 Parameters obtained from the Raman bands of the E-NSGr sample

Sample	G (cm^{-1})	I_G (a.u.)	D (cm^{-1})	I_D (a.u.)	I_D/I_G	L_a (nm)
E-NSGr	1577	1794	1350	1249	0.7	27.2

In order to evaluate the degree of the structural disorder within the E-NSGr sample, the Raman spectrum was also recorded (Fig. 8). Three important bands can be seen in this spectrum: the defect (D) band at 1350 cm^{-1}, the graphite (G) band located at 1577 cm^{-1} and the 2D band at 2700 cm^{-1}.[23]

According to eqn (1), the I_D/I_G ratio may be related to the in-plane crystallite size (L_a), giving an indication of the defect-free domains within the graphene sample:[24]

$$L_a(\text{nm}) = \frac{560}{E_1^4}\left(\frac{I_D}{I_G}\right)^{-1} \tag{1}$$

where E_1 represents the laser excitation energy (2.33 eV) and I_D/I_G is the ratio between the intensity of the D and G bands. The calculated L_a value is around 27 nm (Table 1), confirming that the size of the defect-free domains within the sample is large, therefore the material has a high conductivity.

3.2. Response characteristics of the stochastic biosensors

The response of the stochastic biosensors is based on the channel conductivity: when a constant potential of 125 mV is applied, the current is modified when the molecules of D- or L-aspartic acid enter the channel. In order for the enantiomers to be recognized, two phases need to be completed. During the pattern recognition phase, also known as the first phase, the enantiomers are extracted into the channel, blocking it, the intensity of the current drops to zero until the whole molecules enter the channel; the time spent at this phase is known as t_{off} and represents the signature of the analyte; its value is used for the qualitative analysis of the enantiomers. The binding phase, also known as the second phase,[18-20] takes place when the

Table 3 Recovery tests of L- and D-aspartic acid in biological samples ($N = 10$)[a]

L : D (mol:mol) Stochastic biosensor based on E-NSGr and	1 : 99	1 : 1	99 : 1
	%, Recovery		
Whole blood			
α-Hemolysin	99.83 ± 0.03	99.54 ± 0.05	99.90 ± 0.03
Hemin	99.64 ± 0.05	99.70 ± 0.07	99.81 ± 0.08
Saliva			
α-Hemolysin	99.76 ± 0.04	99.81 ± 0.03	99.79 ± 0.05
Hemin	99.80 ± 0.08	99.83 ± 0.07	99.93 ± 0.05
Urine			
α-Hemolysin	99.84 ± 0.04	99.97 ± 0.02	99.95 ± 0.03
Hemin	99.81 ± 0.09	99.80 ± 0.05	99.76 ± 0.06
Tissue			
α-Hemolysin	99.57 ± 0.02	99.76 ± 0.04	99.89 ± 0.03
Hemin	99.53 ± 0.05	99.85 ± 0.06	99.85 ± 0.03

[a] All results are expressed in μmol L^{-1}.

analytes of interest interact with the wall channel and redox processes take place.

The response characteristics of the proposed stochastic biosensors used for the enantioanalysis of D- and L-aspartic are shown in Table 2. The signatures obtained for the enantiomers of Asp (the t_{off} values) had different values (for the same biosensors) showing that the biosensors are enantioselective. Accordingly, the proposed biosensors are enantioselective, and can be used for the enantioanalysis of aspartic acid.

The linear concentration ranges recorded using the biosensors covered the healthy patients, the asymptomatic patients, as well as patients in different stages of gastric cancer. Accordingly, they can be used for the screening tests of healthy, asymptomatic and clinically ill patients.

The lowest limit of determination for L-Asp as well as the highest sensitivity were obtained for the biosensor based on α-hemolysin. The lowest limit of determination for D-Asp as well

Table 2 Response characteristics of the stochastic biosensors used for the enantioanalysis of aspartic acid

Biosensor based on E-NSGr and	Calibration equation and correlation coefficient (r)[a]	Linear concentration range (mol L^{-1})	t_{off} (s)	Sensitivity (s^{-1}/mol L^{-1})	Limit of determination (mol L^{-1})
α-Hemolysin					
L-Asp	$1/t_{on} = 0.01 + (7.58 \pm 0.03) \times 10^{11} \times C$, $r = 0.9999$	1.0×10^{-15} to 1.0×10^{-3}	0.7 ± 0.01	7.58×10^{11}	1.0×10^{-15}
D-Asp	$1/t_{on} = 0.02 + (1.16 \pm 0.03) \times 10^{2} \times C$, $r = 0.9999$	1.0×10^{-6} to 1.0×10^{-2}	2.0 ± 0.01	1.16×10^{2}	1.0×10^{-6}
Hemin					
L-Asp	$1/t_{on} = 0.06 + (3.75 \pm 0.02) \times 10^{4} \times C$, $r = 0.9999$	1.0×10^{-8} to 1.0×10^{-3}	0.6 ± 0.01	3.75×10^{4}	1.0×10^{-8}
D-Asp	$1/t_{on} = 0.03 + (3.04 \pm 0.02) \times 10^{5} \times C$, $r = 0.9991$	1.0×10^{-9} to 1.0×10^{-3}	1.8 ± 0.02	3.04×10^{5}	1.0×10^{-13}

[a] $1/t_{on} = $ s^{-1}, $C = $ mol L^{-1}.

Table 4 Enantioanalysis of aspartic acid in biological samples from confirmed patients with gastric cancer ($N = 10$)

Sample no.	Enantiomer of aspartic acid[a]	Stochastic biosensor based on E-NSGr and	
		α-Hemolysin	Hemin
Whole blood			
1	L	20.74 ± 0.05	20.26 ± 0.08
	D	108.77 ± 0.02	109.81 ± 0.07
2	L	25.27 ± 0.03	26.95 ± 0.07
	D	87.76 ± 0.03	86.96 ± 0.09
3	L	92.34 ± 0.04	92.37 ± 0.07
	D	225.40 ± 0.02	224.97 ± 0.08
4	L	39.54 ± 0.03	38.24 ± 0.07
	D	157.78 ± 0.05	153.67 ± 0.09
5	L	22.37 ± 0.05	20.26 ± 0.08
	D	40.74 ± 0.08	42.62 ± 0.05
Saliva			
1	L	53.84 ± 0.02	52.12 ± 0.08
	D	41.40 ± 0.03	43.35 ± 0.06
2	L	39.54 ± 0.02	39.25 ± 0.04
	D	18.69 ± 0.04	19.28 ± 0.07
3	D	16.74 ± 0.03	14.21 ± 0.09
	D	33.12 ± 0.02	33.54 ± 0.08
4	L	12.29 ± 0.03	11.41 ± 0.07
	D	40.74 ± 0.03	42.65 ± 0.08
5	L	35.84 ± 0.04	35.48 ± 0.07
	D	22.52 ± 0.03	21.80 ± 0.07
Urine			
1	L	22.37 ± 0.04	21.25 ± 0.08
	D	55.34 ± 0.03	54.01 ± 0.05
2	L	23.16 ± 0.05	23.81 ± 0.07
	D	18.55 ± 0.03	18.39 ± 0.09
3	L	9.80 ± 0.04	10.84 ± 0.08
	D	18.04 ± 0.02	18.50 ± 0.07
4	L	10.26 ± 0.03	10.98 ± 0.05
	D	33.11 ± 0.02	32.78 ± 0.09
5	L	21.59 ± 0.02	20.63 ± 0.07
	D	10.71 ± 0.02	10.21 ± 0.08
Tissue			
1	L	15.64 ± 0.03	16.71 ± 0.07
	D	28.15 ± 0.05	28.79 ± 0.08
2	L	19.55 ± 0.02	18.80 ± 0.09
	D	13.16 ± 0.04	14.88 ± 0.08
3	L	40.43 ± 0.04	40.33 ± 0.07
	D	13.17 ± 0.02	13.21 ± 0.06
4	L	33.49 ± 0.03	32.96 ± 0.08
	D	18.85 ± 0.02	18.40 ± 0.07
5	L	79.80 ± 0.03	77.90 ± 0.09
	D	69.02 ± 0.02	66.07 ± 0.07

[a] All results are expressed in μmol L^{-1}.

Table 5 Enantioanalysis of aspartic acid in whole blood samples from healthy patients ($N = 10$)

Sample no.	Enantiomer of aspartic acid[a]	Stochastic biosensor based on E-NSGr and	
		α-Hemolysin	Hemin
1	L	331.10 ± 0.03	332.48 ± 0.07
2	L	167.43 ± 0.02	165.23 ± 0.09
3	L	615.53 ± 0.02	613.55 ± 0.08
4	L	162.47 ± 0.04	167.10 ± 0.08
5	L	215.92 ± 0.03	213.74 ± 0.07

[a] All results are expressed in μmol L^{-1}

the first day of utilization for screening tests of biological samples.

3.3. Selectivity and enantioselectivity of the stochastic biosensors

The selectivity of the stochastic biosensors is given by the signatures obtained for different biomarkers or substances determined with the same biosensor; differences in the values recorded for the main analyte and other substances means selectivity. Different signature values for D- and L-aspartic acid were obtained for the proposed stochastic biosensor proving their enantioselectivity (Table 2). The selectivity of the biosensors were checked *versus* other aminoacids: histidine, lysine, glutamine, serine, triptophane, arginine, and alanine. For the signature of these aminoacids, values higher than 2.0 were recorded (histidine 2.3, lysine 2.8, glutamine 2.1, serine 2.5, triptophane 3.2, arginine 3.5, and alanine 3.0), proving that the biosensors are selective.

3.4. Analytical applications

The determination of the enantiomers in biological samples (whole blood, urine, saliva, and tissue) was done in accordance with the procedure described in the stochastic mode: the signatures of the two enantiomers were identified in the diagrams (Fig. 2 and 3), and the t_{on} values were read and used for the calculation of the concentrations of the enantiomers.

The validation of the proposed stochastic biosensors was done in two steps. During the first step, recovery tests were performed. Whole blood samples from healthy patients were spiked with L- and D-Asp, after an initial screening test, when the amounts of L- and D-Asp were determined. The results shown in Table 3 proved that the recovery of the enantiomers is higher than 95.00% in the biological samples (whole blood, urine, saliva, tissue), with RSD values lower than 1.00%.

The second stage of validation was done using real samples of whole blood from healthy patients, and of whole blood, urine, saliva, and tissue samples from confirmed patients with gastric cancer.

The results shown in Tables 4 and 5 proved a good correlation between the concentrations obtained using the two biosensors. While in the case of the confirmed patients with

as the highest sensitivity were obtained for the biosensor based on hemin.

The proposed biosensors were tested daily for a period of 6 months. During this period of time, their sensitivities did not change with more than 1.00% from the values measured in

gastric cancer, both enantiomers L- and D- of Asp were identified and quantified (Table 3), for healthy patients, only L-Asp was identified and quantified (Table 5). Accordingly, this test may be used for fast screening of biological samples, contributing to a fast and in some cases early diagnosis of gastric cancer and neuroendocrine or neurodegenerative diseases.

4. Conclusions

Two stochastic biosensors based on the immobilization of α-hemolysin and hemin in the paste of an exfoliated graphene doped with N and S were used for the enantioanalysis of aspartic acid in biological samples: whole blood, urine, saliva, and tissue. The proposed stochastic biosensors showed high sensitivity, low limits of determination, and high selectivity and enantioselectivity. The results obtained for the validation of the screening test showed that the proposed biosensors and test can be used for the enantioanalysis of aspartic acid in biological samples, and also for the fast detection of gastric cancer.

Funding

Author contributions

Conceptualization, R. I. S. v. S., S. M. P., R. M. I. M.; methodology, R. I. S. v. S., D. C. G., R. M. I. M., and L. B. T.; validation, R. I. S. v. S., D. C. G., and R. M. I. M.; investigation, D. C. G., L. B. T. and R. M. I. M.; writing—original draft preparation, R. I. S. v. S., D. C. G., R. M. I. M., S. M. P. and L. B. T.; writing—review and editing, R. I. S. v. S., D. C. G., R. M. I. M., S. M. P. and L. B. T.; supervision, R. I. S. v. S. All authors have read and agreed to the published version of the manuscript. The authors are grateful to Dr Bogdan Cozar for the Raman investigation of the graphene sample and to Dr Irina Kacso for the FTIR investigation and useful discussions regarding the spectrum interpretation.

Conflicts of interest

The authors declare no conflict of interest. The funders had no role in the design of the study; in the collection, analyses, or interpretation of data; in the writing of the manuscript, or in the decision to publish the results.

Acknowledgements

References

1 J. Liu, S. Lin, Z. Li, L. Zhou, X. Yan, Y. Xue, L. Meng, J. Lu, B. Suo and W. Jiang, Free amino acid profiling of gastric juice as a method for discovering potential biomarkers of early gastric cancer, *Int. J. Clin. Exp. Pathol.*, 2018, **11**, 2323–2336.

2 J. J. A. J. Bastings, H. M. van Eijk, S. W. O. Damink and S. S. Rensen, D-amino acids in health and disease: a focus on cancer, *Nutrients*, 2019, **11**, 2205.

3 S. Ritz-Timme and M. J. Collins, Racemization of aspartic acid in human proteins, *Ageing Res. Rev.*, 2002, **1**, 43–59.

4 A. D'Aniello, D-aspartic acid: an endogenous amino acid with an important neuroendocrine role, *Brain Res. Rev.*, 2007, **53**, 215–234.

5 S. Xiao and L. Zhou, Gastric cancer: metabolic and metabolomics perspectives (review), *Int. J. Oncol.*, 2017, **51**, 5–17.

6 A. N. Fonteh, R. J. Harrington, A. Tsai, P. Liao, M. G. Harrington, *et al.*, Free amino acid and dipeptide changes in the body fluids from Alzheimer's disease subjects, *Amino Acids*, 2007, **32**, 213–224.

7 S. Nishiumi, T. Kobayashi, A. Ikeda, *et al.*, A novel serum metabolomics-based diagnostic approach for colorectal cancer, *PLoS One*, 2012, **7**, e40459.

8 B. S. Sekhon, Enantioseparation of chiral drugs—an overview, *Int. J. Pharm. Technol. Res.*, 2010, **2**, 1584–1594.

9 P. K. Katiyar and R. K. Wala, Chiral separation of aspartic acid by thin layer chromatography, *Asian J. Chem.*, 2010, **22**, 4945–4946.

10 P. J. van den Oetelaar, L. E. van Beijsterveldt, J. R. van Beckhoven and H. J. Hoenders, Detection of aspartic acid enantiomers by chiral capillary gas chromatography. Determination of in vivo racemisation and reduction of metal-induced background, *J. Chromatogr. A*, 1986, **386**, 135–143.

11 H. Yu, Y. S. Ding and S. F. Mou, Some factors affecting separation and detection of amino-acids by high performance anion-exchange chromatography with integrated pulsed amperometric detection, *J. Chromatogr. A*, 2003, **997**, 145–153.

12 S. Wang, L. Fan and S. Cui, CE-LIF chiral separation of aspartic acid and glutamic acid enanatiomers using human serum albumin and sodium cholate as dual selectors, *J. Sep. Sci.*, 2009, **32**, 3184.

13 H. Guan, P. Zhou, X. Zhou and Z. He, Sensitive and selective detection of aspartic acid and glutamic acid based on polythiophene-gold nanoparticles composites, *Talanta*, 2008, 77, 319–324.

14 Y. H. Deng, H. Wang and H. S. Zhang, Determination of amino acid neurotransmitters inhuman cerebrospinal fluid and saliva by capillary electrophoresis with laser-induced fluorescence detection, *J. Sep. Sci.*, 2008, **31**, 3088–3097.

15 B. B. Prasad, A. Srivastava and M. P. Tiwari, Highly sensitive and selective hyphenated technique (molecularly imprinted polymer solid-phase microextraction–molecularly imprinted

polymer sensor) for ultra trace analysis of aspartic acid enantiomers, *J. Chromatogr. A*, 2013, **1283**, 9–19.

16 G. Herzog and D. W. Arrigan, Electrochemical strategies for the label-free detection of amino acids, peptides and proteins, *Analyst*, 2007, **132**, 615–632.

17 P. Jainish and P. Prittesh, Biosensors and biomarkers: promising tools for cancer diagnosis, *Int. J. Biosens. Bioelectron.*, 2017, **3**, 313–316.

18 R. I. Stefan-van Staden, I. Popa-Tudor, C. I. Tirgoviste and R. A. Stoica, Molecular Recognition and Determination of Interleukins 1β, 6, 12, and 17 in Whole Blood from Diabetic Patients, *Anal. Lett.*, 2020, **53**, 2021–2033.

19 R. I. Stefan-van Staden, A. Moscalu-Lungu and M. Badulescu, Disposable Stochastic Sensors Based on Nanolayer Deposition(s) of Silver, and AgC Composite on Plastic for the Assay of α-Amylase in Whole Blood and Saliva, *Nanomaterials*, 2020, **10**, 1528.

20 R. I. Stefan-van Staden, D. C. Gheorghe, V. Jinga, C. S. Sima and M. Geanta, Fast Screening of Whole Blood and Tumor Tissue for Bladder Cancer Biomarkers Using Stochastic Needle Sensors, *Sensors*, 2020, **20**, 2420.

21 F. Pogacean, M. Coros, L. Magerusan, V. Mirel, A. Turza, G. Katona, R. I. Stefan-van Staden and S. Pruneanu, Exfoliation of graphite rods *via* pulses of current for graphene synthesis: Sensitive detection of 8-hydroxy-2-deoxyguanosine, *Talanta*, 2019, **196**, 182–190.

22 R. A. Rochman, S. Wahyuningsih, A. H. Ramelan and Q. A. Hanif, Preparation of nitrogen and sulphur Co-doped reduced graphene oxide (rGO-NS) using N and S heteroatom of thiourea, *IOP Conf. Ser.: Mater. Sci. Eng.*, 2019, **509**, 012119, DOI: 10.1088/1757-899X/509/1/012119.

23 A. C. Ferrari and D. M. Basko, Raman spectroscopy as a versatile tool for studying the properties of graphene, *Nat. Nanotechnol.*, 2013, **8**, 235–246.

24 L. G. Caņado, K. Takai, T. Enoki, M. Endo, Y. A. Kim, H. Mizusaki, A. Jorio, L. N. Coelho, R. Magalhães-Paniago and M. A. Pimenta, General equation for the determination of the crystallite size L_a of nanographite by Raman spectroscopy, *Appl. Phys. Lett.*, 2006, **88**, 1–4.